Food Research International 105 (2018) 637–644

Contents lists available at ScienceDirect

Food Research International

journal homepage: www.elsevier.com/locate/foodres

Incorporation of bentonite clay in cassava starch films for the reduction of water vapor permeability

M.K.S. Monteiro[a], V.R.L. Oliveira[b,*], F.K.G. Santos[b], E.L. Barros Neto[a], R.H.L. Leite[b], E.M.M. Aroucha[b], R.R. Silva[a], K.N.O. Silva[a]

[a] Universidade Federal do Rio Grande do Norte, UFRN, Natal, RN 59.078-970, Brazil
[b] Universidade Federal Rural do Semi-Árido, UFERSA, Mossoró, RN 59.625-900, Brazil

ARTICLE INFO

Keywords:
Modified clay
Glycerol
Cassava starch
Biofilm
Water vapor permeability
Factorial planning

ABSTRACT

Complete factorial planning 2^3 was applied to identify the influence of the cassava starch(A), glycerol(B) and modified clay(C) content on the water vapor permeability(WVP) of the cassava starch films with the addition of bentonite clay as a filler, its surface was modified by ion exchange from cetyltrimethyl ammonium bromide. The films were characterized by X-ray diffraction(XRD), fourier transform by infrared radiation(FTIR), atomic force microscopy(AFM) and scanning electron microscopy(SEM). The factorial analysis suggested a mathematical model thats predicting the optimal condition of the minimization of WVP. The influence of each individual factor and interaction in the WVP was investigated by Pareto graph, response surface and the optimization was established by the desirability function. The sequence of the degree of statistical significance of the investigated effects on the WVP observed in the Pareto graph was C > B > A > BC > AC. Interactions AB, BC and AC showed that the modified clay was the factor of greater significance.

1. Introduction

Recent decades have witnessed a growing interest in the development of biopolymeric films designed to reduce environmental pollution caused by non-degradable waste from synthetic polymers, mostly derived from petroleum. To compete with these conventional materials, biopolymers, which are biodegradable materials from renewable sources, can be a healthy alternative to reduce this negative impact on society (Restrepo-Flórez, Bassi, & Thompson, 2014).

Besides the sustainable character, there is also interest in the food industry to use biodegradable films as a coating of fresh fruits and vegetables, due to the intense demand for products in good conditions of consumption. For this, biopolymers must have their physicochemical properties modified, since their hydrophilic nature influences the barrier properties of the coating (Reddy, Vivekanandhan, Misra, Bhatia, & Mohanty, 2013; Rhim, Park, & Hac, 2013). Therefore, the demand for an edible coating that is sustainable and with excellent water vapor barrier, mechanical, optical and thermal properties is a challenge.

In this context, the biodegradable films with excellent barrier properties used for fruit coatings play an important role in the preservation, distribution and commercialization of these films, since it is able to reduce respiration and the production of ethylene by the product, besides carrying chemical additives that help in the maintenance of quality and that reduce the deterioration by microorganisms, actually prolonging shelf life of the fruits, once reduced mainly due to storage in a high humidity environment (Azarakhsha, Osmana, Ghazalia, Tanb, & Mohd Adzahanb, 2014; Cortez-Vega, Pizato, Souza, & Prentice, 2014; Pascall & Lin, 2013; Velickova, Winkelhausen, Kuzmanova, Moldao-Martins, & Alves, 2013).

The main substances used as forming a biopolymeric matrix are proteins, alginates, pectins, starches, cellulose derivatives and other polysaccharides (Wihodo & Moraru, 2013). Cassava starch is a polysaccharide synthesized by plants to be used as an energy reserve and is considered one of the most promising natural biopolymers because of its attractive combination of high availability, biodegradability and relatively low cost (Zhu, 2015). However, cassava starch due to its hydrophilic structure resulting from the presence of amylose and amylopectin in its composition requires that its water vapor barrier properties be improved (Romero-Bastida, Bello-Pérez, Velazquez, & Alvarez-Ramirez, 2015).

Studies have been carried out on the addition of clay in the formation of bionanocomposite films, where the degree of clay dispersion along the biopolymeric matrix may be related to the improvement of the water vapor barrier property of the original biofilm (Souza et al., 2012). This may be due to the clay when modified in the presence of a surfactant to add hydrogen bonds to the structure of the biopolymer

* Corresponding author.
E-mail addresses: mayra.kerolly@gmail.com (M.K.S. Monteiro), vrafaeloliveira@uol.com.br (V.R.L. Oliveira).

https://doi.org/10.1016/j.foodres.2017.11.030
Received 18 May 2017; Received in revised form 15 November 2017; Accepted 19 November 2017
Available online 02 December 2017
0963-9969/ © 2017 Elsevier Ltd. All rights reserved.

matrix, thus contributing to the permeation resistance of water vapor molecules (Tan & Thomas, 2016). Thus, it is important for thermoplasticization of the biopolymer responsible to increase or reduce such aggregation depending on the concentration of plasticizer (Chivrac, Pollet, Dole, & Avérous, 2010; Muller, Laurindo, & Yamashita, 2011).

Other studies have investigated the contribution of clay treatment to biopolymeric films (Alboofetileh, Rezaei, Hosseini, & Abdollahi, 2013; Casariego et al., 2009; Lavorgna, Piscitelli, Mangiacapra, & Buonocore, 2009; Qi, Li, Sun, Shi, & Wang, 2016; Rhim et al., 2013). A complete 2^3 factorial design involving the factors and their interactions that can influence the physical-chemical properties of the original biofilm was not carried out. Thus, the objective of this work was to investigate the individual and interactive effects of the addition of modified bentonite clay and the concentrations of plasticizer and biopolymer on the water vapor permeability rate of cassava starch films.

2. Materials and methods

2.1. Materials

Was used in the preparation of films, cassava starch, of the Indústria Primícias do Brasil, Macaíba, RN, Brazil. The calcium bentonite clay (Bent-Ca) used was kindly supplied by Armil Mineração Nordeste (AMN), Parelhas, RN, Brazil, with a mean particle size of 0.074 mm and a cation exchange capacity equal to 90 mmol/100 g. Surface modification of the clay was performed in the presence of cetyltrimethyl ammonium bromide (CTAB), manufactured by Sigma Life Science, USA, in 98% purity. The alcohol used was ethyl alcohol (95.5°GL Absolute) of the brand Synth, produced in Diadema, SP, Brazil. Glycerol PA (Synth) was used as plasticizer.

2.2. Modification of clay

To obtain the organophilized calcium bentonite clay (OBent-Ca), a suspension of 1% by mass of Bent-Ca in deionized water was initially prepared. This solution was kept under stirring at 30 °C in a thermostat. In another container, the CTAB was dissolved in 20 mL of ethyl alcohol to form a 0.06 M solution. The two blends were then homogenized and kept under stirring for 12 h at 30 °C. After stirring, the mixture was filtered and washed to remove excess salt. The material trapped in the filtration was brought to the oven at 60 °C and held for 24 h. After drying, they were macerated with mortar and pistil, and then sieved in ABNT No. 200 sieve (φ = 0.074 mm) (Lee, Park, Kim, Kim, & Park, 2014).

The elemental composition of Bent-Ca and OBent-Ca was characterized by X-ray fluorescence (XRF) and the result is listed in Table 1.

2.3. Preparation of films

Were prepared 11 filmogenic solutions with 0 g until 5 g of cassava starch. Between 0% and 5% of OBent-Ca and 10% to 30% of glycerol were used, each percentage being in relation to the dry mass of cassava starch. The deionized water was the solvent used for the formation of each filmogenic solution, which were obtained from stirring with heating at 70 °C in a thermosetter for 15 min. After preparation, filmogenic solutions were placed 80 mL in rectangular plates of 23 cm × 13 cm × 2 cm, and the solutions were dried at 40 °C for 6 h (Cyras, Manfredi, Minh-Tan, & Vazquez, 2008).

2.4. Characterization

2.4.1. Thickness

The thicknesses of the films were measured using a Mitutoyo micrometer (Model MDC-25M, MFG/Japan). The measurements were taken at five different points throughout the film.

2.4.2. X-ray diffraction – XRD

The XRD analyzes were conducted at room temperature on a Shimadzu DRX-6000 equipment, using Cukα radiation (λ = 1.5418 Å), a voltage of 40 kV and a current of 30 mA. The samples were analyzed in a range of 2θ between 2 and 30° with a scan speed of 2°/min.

2.4.3. Fourier transform infrared spectroscopy – FTIR

The infrared absorption spectra were obtained with a Shimadzu IRTracer-100 spectrometer, scanning from 7800 to 350 cm^{-1} and 4 cm^{-1} resolution. The samples were characterized directly by attenuated total reflectance, without any type of preparation.

2.4.4. Atomic force microscopy – AFM

The morphological surface of the films was analyzed using a Shimadzu atomic force microscope, Model SPM-9700. The analysis was performed in a tapping mode with a scanning speed of 1 Hz. No treatment was done on the sample for analysis.

2.4.5. Scanning electronic microcopy – SEM

The samples were submitted to the SEM (model VEGA 3 TM, TESCAN-Czech Republic, 2013) applied at a voltage of 15 kV, with a magnitude of 1 kx.

2.4.6. Water vapor permeability - WVP

The water vapor permeability of the films was determined gravimetrically (ASTM method E96-93; Monteiro et al., 2017). The films were cut into square pieces (2 cm × 2 cm) and sequentially deposited on top of the WVP measuring cells. The water level was up to 1 cm below the film. The weight of each cell was measured before being deposited in a desiccator which contained silica stones at the bottom, as well as a relative humidity of 50% and internal temperature of 29 °C. Cell weight was measured every hour over a period of 8 h. The WVP of the films was calculated in g.mm/kPa.m^2.h as follows in Eq. 1:

$$WVP = \frac{W \cdot L}{A \cdot t \cdot \Delta P} \quad (1)$$

where W is the weight of water permeating through the film (g); L is the film thickness (mm); A is the permeation area (m^2); t is the permeation time (h); ΔP is the pressure difference to water vapor between the two sides of the film (kPa).

2.5. Statistical analysis

Table 2 shows the limits used for each variable, cassava starch mass and percentages of glycerol and OBent-Ca in relation to the dry mass of biopolymer used, established by previous studies (Chivrac et al., 2010; Coativy et al., 2015; Cyras et al., 2008; Gao et al., 2014; Liu, Chaudhary, Yusa, & Tadé, 2011; Matsuda, Verceheze, Carvalho,

Table 1
Elementary composition of Bent-Ca and OBent-Ca.

	Elements	Si	Al	Fe	Ca	Mg	K	Br	Others
Mass (%)	Bent-Ca	53.8943	15.7085	12.1755	10.1266	2.8674	1.6885	–	3.5392
	OBent-Ca	50.5182	23.5318	8.0187	6.6768	1.6831	1.0515	8.5199	–

Table 2
Minimum and maximum levels and central point of the three factors investigated.

Factors	Minimum level	Central point	Maximum level
Cassava starch (g)	2	3.5	5
Glycerol (%)	10	20	30
OBent-Ca (%)	0	2.5	5

Yamashita, & Mali, 2013; Muller et al., 2011; Romero-Bastida et al., 2015; Romero-Bastida, Tapia-Blácido, Méndez-Montealvo, Velázquez, & Ramirez, 2016; Souza et al., 2012; Xie, Pollet, Halley, & Avérous, 2013; Zhu, 2015). The WVP was determined with the average of three experiments in parallel. The order in which experiments were performed was random to avoid systematic errors. The results were analyzed with Statistica 8 software, and the main effects and interactions between factors were determined. The central point was adopted to verify the error of the model, being realized in triplicate.

3. Results and discussion

3.1. Factorial analysis

The development of a mathematical model, based on experimental planning, is used in this work with the objective of optimizing the water vapor barrier property of the cassava starch film. This model predicts the behavior of the water vapor permeability rate of the ideal cassava starch film, that is, with the lowest WVP rate, based on experimental data collected in the laboratory. A complete factorial design 2^3 was used for this purpose. Thus, the influence of the three factors selected as important for measuring the desired response variable was evaluated with satisfactory statistical reliability. Table 3 shows the experimental points of the planning each with their respective response and composition coded. Table 4 shows the effects of each factor and interaction, the correlation coefficients of the mathematical model and the statistical parameters that demonstrate the significance of the effects investigated in WVP.

In this sense, it was observed, according to the statistical parameters shown in Table 4, that the individual effects of cassava starch and glycerol significantly influence the increase of the WVP of the biofilm. This is due to the fact that cassava starch has an extensive monomer chain formed by hydrocarbons and branched by hydroxyl groups from the predominance of amylopectin in its composition (Romero-Bastida et al., 2016; Zhu, 2015). As for glycerol, the effect is observed from the thermoplasticization, where, due to its highly hydrophilic characteristics, such plasticizer promotes the starch film to break the internal hydrogen bonds and the intermolecular and intramolecular attraction forces established between the biopolymer chains, resulting in the increase of the intermolecular space that propitiates the vulnerability of the biopolymeric matrix in establishing connections with the molecules of water vapor (Chivrac et al., 2010).

Table 4
Estimated effects of the three investigated factors, the correlation coefficients of the model and the statistical parameters for the WVP response.

Parameters	Effects	Correlation coefficient	Default error	T–value	P–value
Mean	0.50569	0.50569	0.001740	290.6281	0.00001
Cassava Starch (1)	0.08230	0.04115	0.002040	20.1684	0.00245
Glycerol (2)	0.16350	0.08175	0.002040	40.0682	0.00062
OBent-Ca (3)	− 0.31875	− 0.15937	0.002040	− 78.1126	0.00016
1*2	0.01330	0.00665	0.002040	3.2593	0.08263
1*3	− 0.02585	− 0.01292	0.002040	− 6.3348	0.02402
2*3	− 0.05135	− 0.02567	0.002040	− 12.5838	0.00626
1*2*3	− 0.00415	− 0.00207	0.002040	− 1.0170	0.41616

In this perspective, the individual effects of the three factors were significant on WVP, and OBent-Ca is the factor that contributes to the improvement of the water vapor barrier property of the cassava starch film. This fact can be explained by the fact that Bent-Ca in its natural state is a hydrophilic mineral because it presents a stacked structure of silicate layers interconnected by Van der Waals forces due to the presence of free inorganic cations in the called interlamellar galleries (Coativy et al., 2015; Monteiro et al., 2017). Knowing this, Bent-Ca can undergo a chemical modification process on its surface, where its exchangeable calcium cations are replaced by the quaternary ammonium salt, making it organophilic and, consequently, electrostatically compatible with the cassava starch matrix. This occurs because the salt has an extensive carbon chain that promotes a basal space between the silicate layers, resulting in space for the biopolymer to interlace between the electronegative tail of the surfactant, so OBent-Ca is dispersed evenly along the matrix of starch, and makes the way for the passage of water vapor molecules tortuous. In this sense, it occurs the reduction of the diffusion of these molecules and, consequently, an improvement in the water vapor barrier property of the original biofilm (Chiu, Huang, Wang, Alamani, & Lin, 2014; Gao et al., 2014; Kotal & Bhowmick, 2015; Muller et al., 2011).

In terms of the interaction between two factors, the interactions of OBent-Ca with both cassava starch and with glycerol were significant for WVP reduction. This may be a consequence of the range of glycerol content investigated to make cassava starch more compatible electrostatically to the functional groups of the surfactant present in the OBent-Ca interlayer galleries (Lavorgna et al., 2009; Souza et al., 2012). The interaction between starch and glycerol as well as the interaction between the three factors were neglected because they did not significantly influence the response of the WVP, and the observed can be due to the diffusion coefficient of the water vapor molecules through

Table 3
Experimental points and their encodings used in the experimental design and their respective WVP responses.

Test	Real value			Encoded value			Response
	Cassava starch (g)	Glycerol (%)	OBent-Ca (%)	Cassava starch	Glycerol	OBent-Ca	WVP (g·mm/KPa·m^2·h)
1	2	10	0	− 1	− 1	− 1	0.5141
2	5	10	0	1	− 1	− 1	0.6048
3	2	30	0	− 1	1	-1	0.7115
4	5	30	0	1	1	-1	0.8371
5	2	10	5	-1	-1	1	0.2684
6	5	10	5	1	-1	1	0.3157
7	2	30	5	-1	1	1	0.3714
8	5	30	5	1	1	1	0.437
9	3.5	20	2.5	0	0	0	0.5075
10	3.5	20	2.5	0	0	0	0.497
11	3.5	20	2.5	0	0	0	0.4981

the biopolymeric matrix depend on the concentration of glycerol and relative air humidity (Muller et al., 2011; Tan & Thomas, 2016).

Therefore, factorial analysis results in Eq. (2) that corresponds to a mathematical model of linear regression that predicts the water vapor permeability rate of cassava starch films as a function of each of the factors investigated in the experimental planning.

$$WVP = 0.50645 + 0.04115X_1 + 0.08175X_2 - 0.15937X_3 - 0.01292X_1X_3 - 0.02567X_2X_3 \quad (2)$$

where X_1, X_2 and X_3 correspond to the variables of the codified factors, cassava starch, glycerol and OBent-Ca, respectively.

Moreover, the reliability of this mathematical model was tested through statistical analyzes, such as Student's *t*-test, ANOVA and normal probability graph, and its effects on the response variable interpreted by Pareto Graph and response surface. The results of the factorial planning for the optimization of the factors to obtain the lowest water vapor permeability rate of the cassava starch film were evidenced by the desirability function.

3.1.1. ANOVA

In order to ensure an appropriate predictive model, the mathematical model regression test was performed by applying analysis of variance (ANOVA) (Abdel-Ghani, Hegazy, El-Chaghaby, & Lima, 2009; Palanikumara & Davim, 2009). Table 5 shows the quadratic sum, degree of freedom and the mean square of both the regression and the residue used for the F test. Thus, the $F_{cal} = 566.896$ was higher than the tabulated $F_{5\%\ (6.2)} = 19.33$ characterizing model of linear regression as statistically significant. This is verified by ratio $F_{calculated/tabulated} >$ 1(See Table 5). In addition, the regression model is considered useful for prediction purposes, since the value of the calculated F was greater than ten times the value of the tabulated F. The R_2-sqr indicated that the regression model explained 99.941% of the WVP variability, in addition to the adjusted coefficient of determination, $R_{adj}{}^2$.

3.1.2. Pareto graph

Fig. 1 present the Pareto graph showing which of the individual factors analyzed, as well as which interactions between these factors contribute significantly to the WVP of the cassava starch film.

The value of each effect is shown in the Pareto graph by horizontal columns according to Fig. 1, where the dotted vertical line indicates the minimum magnitude in which the effect is statistically significant to the WVP observed at the 95% confidence level (Abdel-Ghani et al., 2009). Thus, the individual effects (starch (1), glycerol (2) and OBent-Ca (3)) and their interactions (1*3 and 2*3) were considered significant because they extend beyond the reference line at the level of 0.05. The Pareto graph also shows that OBent-Ca represents the individual effect with a greater significant load on the WVP, already in relation to the interaction between the two factors is 2*3 that presents this degree of significance. In addition, the 1*2 and 1*2*3 interactions were not significant for 95% confidence WVP. The sequence of the degree of statistical significance on WVP in relation to the effects investigated is therefore OBent-Ca (1) > glycerol (2) > starch (1) > 2*3 > 1*3.

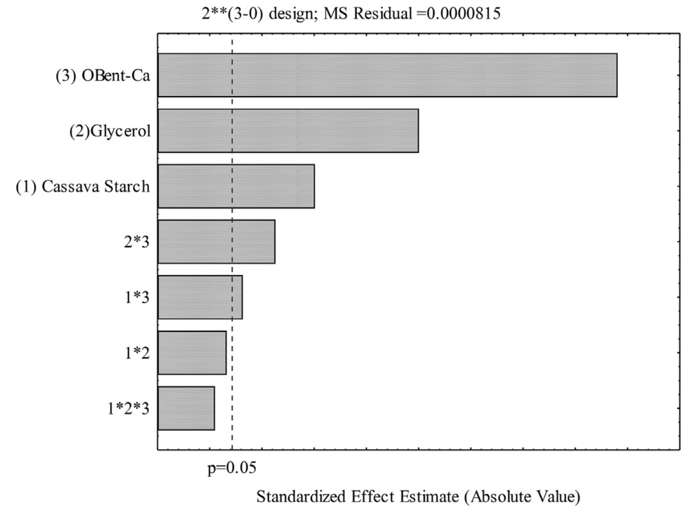

Fig. 1. Pareto graph of standardized effects. Source: own authorship.

These results confirm that the presence of OBent-Ca prevents the diffusion of water vapor molecules along the cassava starch film, both by reducing the vulnerability of the biopolymeric matrix to interact with the moisture difference of the environment, as well as by the formation of a tortuous way somewhat long from the mass transfer zone (Monteiro et al., 2017; Tan & Thomas, 2016).

3.1.3. Response surface

Fig. 2 shows the response surfaces of WVP as a function of the factors, concentration of cassava starch (1), glycerol (2) and OBent-Ca (3).

Only the interactions 1*3 and 2*3 were significantly influenced by the water vapor permeability rate of starch films, since the surfaces of responses of both the interaction 2*3 (Fig. 2a) and the interaction 1*3 (Fig. 2b) presented a considerable slope of the plane, when compared to the interaction 1*2 (Fig. 2c) which resulted only in a slight slope (Bingol, Tekin, & Alkan, 2010; Hank, Azi, Hocine, Chaalal, & Hellal, 2014). The negative effect of starch and glycerol on WVP was more significant at low levels of OBent-Ca, whereas the effect of OBent-Ca was more sensitive to high levels of starch and glycerol, but WVP was lower to the low contents of these, which implies that the high content of OBent-Ca is observed the best property of water vapor barrier. Therefore, the interaction effects between factors 1*3 and 2*3 revealed that the biofilm with the best water vapor barrier property should occur at low levels of cassava starch and glycerol, and high levels of OBent-Ca. These results associate the fact that the OBent-Ca exfoliate along the starch matrix gives a barrier character that reduces the permeability rate to the water vapor of the original film, to the glycerol content used, which makes the biopolymeric matrix more compatible with the functional groups of the surfactant that superficially modified the clay (Chiu et al., 2014; Chivrac et al., 2010). However, in order to observe such an effect the glycerol and the starch must be in low concentrations

Table 5
Analysis of the variance for the adjustment, by the least squares method, of the linear model.

Source of VARIATION	Quadratic sum	N° of degrees of freedom	Quadratic mean	$F_{calculated}$	$F_{tabulated}$	$F_{calculated/tabulated}$
Regression	0.277212	6	0.046202	566.896	19.33	29.3272
Residue	0.000163	2	0.0000815			
Lack of adjustment	0.000096	1	0.000096			
Pure error	0.000067	1	0.000067			
Total	0.277375	8				

$R^2 = 0.99941$; $R^2_{Adj} = 0.99805$; $F_{cal} = MQ_{Regression}/MQ_{residue}$
% of variation explained = 99.94%.
% maximum explanable variation = 99.98%.

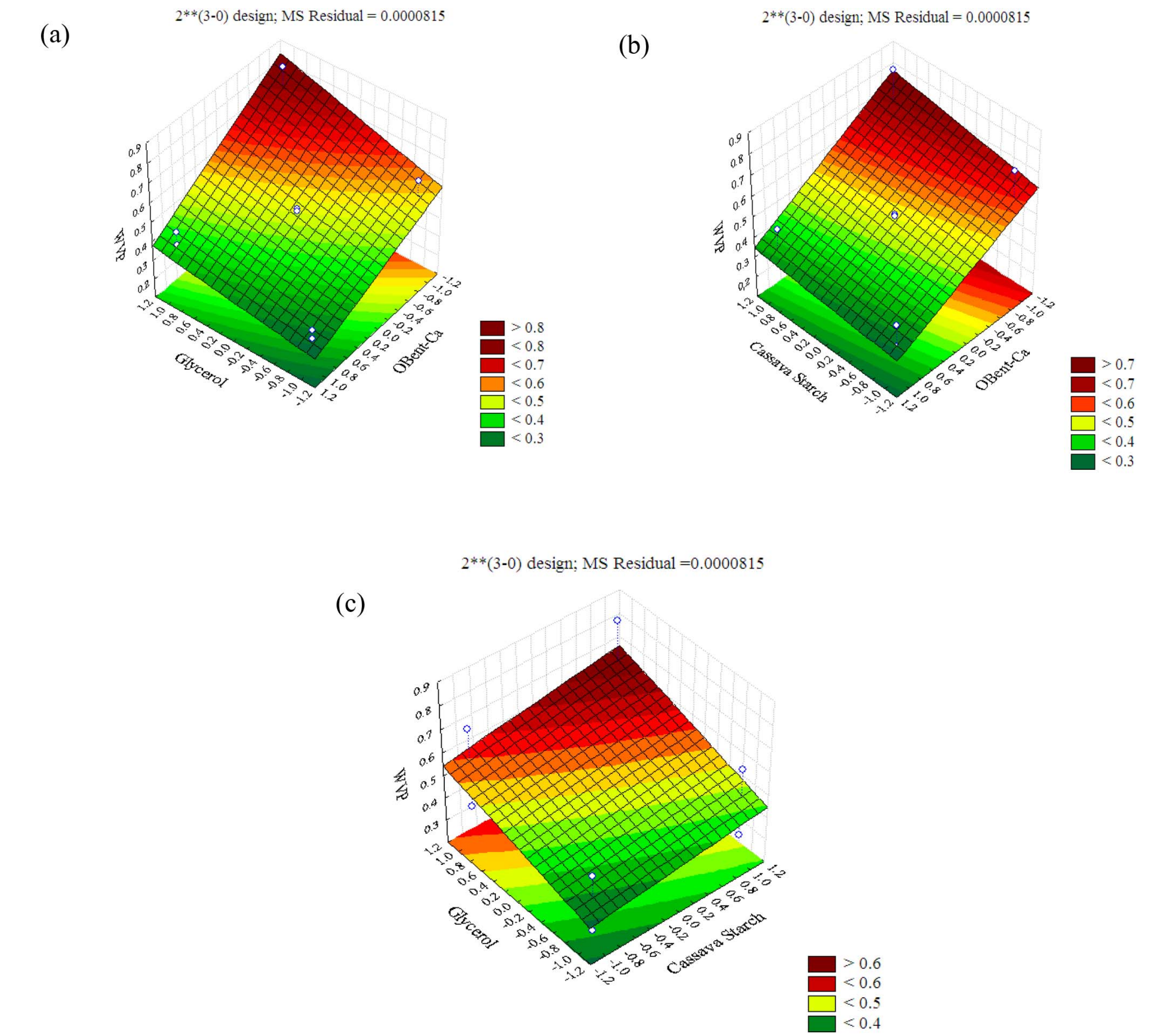

Fig. 2. The response surfaces for the standardized effects of the interaction between: (a) glycerol-OBent-Ca (b) cassava starch-OBent-Ca and (c) cassava starch-glycerol. Source: own authorship.

considering that both are highly hydrophilic.

3.1.4. Estimation of optimal design conditions by the desirable function method

Fig. 3 shows the quantitative measurement of each factor for the determination of the cassava starch films with both the lowest (A) and the highest (B) WVP.

The method of the desirability function, as shown in Fig. 3, was used to identify the cassava starch film with the best water vapor barrier property from the optimization of each factor (Hank et al., 2014). The optimum condition, that is, the best combination of factor configurations characterized the biofilm A with 2 g of cassava starch, 10% of glycerol and 5% of modified clay. In addition, biofilm B was characterized with 5 g cassava starch, 30% glycerol and 0% modified clay. The percentages are in relation to the dry mass of starch used.

3.2. Characterization of cassava starch films with both the lowest and the highest water vapor permeability

3.2.1. X-ray diffraction - XRD

The XRD was performed in order to verify the displacement of the peak corresponding to the plane (001) in OBent-Ca in relation to Bent-Ca, and to study the structural pattern of biofilms A and B. The diffractograms are shown in Fig. 4.

The Bent-Ca standard diffractogram in Fig. 4a identifies at $2\theta = 5.8^{\circ}$ the peak referring to the plane (001) demonstrating the presence of the elements of the silicate layers that compose it, in turn, the diffractogram of OBent-Ca identifies the same peak at $2\theta = 2.4^{\circ}$, and it is then possible to prove the increase of the basal space between such silicate layers. This is due to the superficial modification of the Bent-Ca surface, which changes from hydrophilic to organophilic in the presence of a quaternary ammonium salt, as it replaces the interchangeable inorganic cations present in the interlamellar region responsible for compactibilizing the silicate layers to form a stacking

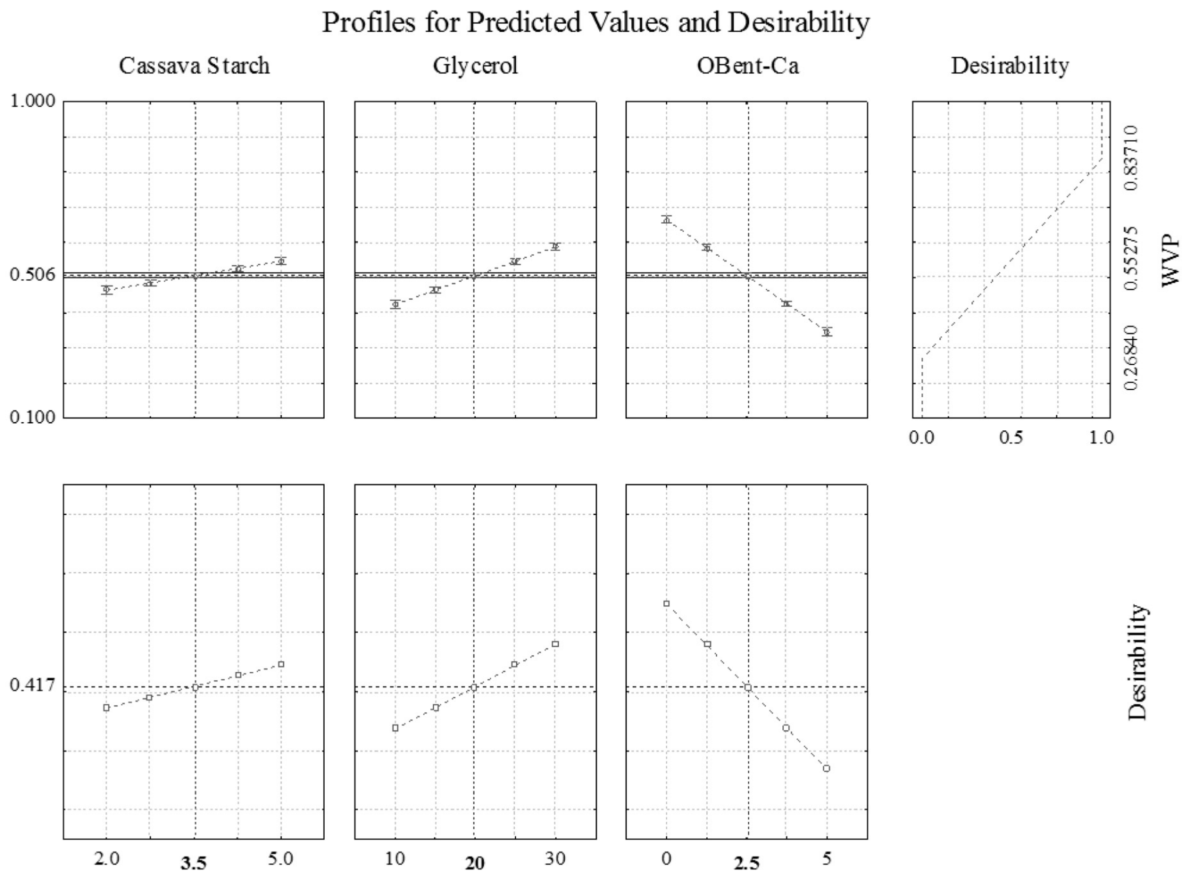

Fig. 3. Desirability function for WVP optimization. Source: own authorship.

(Chiu et al., 2014; Kotal & Bhowmick, 2015).

In Fig. 4b, through the diffractograms of the cassava starch films A and B, it is possible to observe the formation of a bionanocomposite exfoliated in biofilm A, as well as the predominant presence of amylopectin in the structural pattern of the biopolymeric matrix, which proves a semicrystalline structure and of high hydrophilicity. In this perspective, the identification of the peak at $2\theta = 20^{\circ}$ in both diffractograms of the films makes reference to the crystallinity caused by the formation of the granules of cassava starch resulting from the interlacing between the amylose and the amylopectin after the gelatinization process, however, these diffractograms identify in most amorphous regions, since amylopectin has a branched chain structure with crystalline regions alternated by amorphous regions (Gao et al., 2014; Zhu, 2015).

In fact, obtaining a bionanocomposite in biofilm A is evidenced by the exfoliation of the silicate layers along the starch matrix, since the peak referring to the plane (001) can be located at angles of diffraction smaller than that identified in the diffractogram Of Bent-Ca (Fig. 4b). This exfoliation occurs due to the fact that OBent-Ca provides space and compatibility to the starch that intertwines among the silicate layers dispersing them evenly, as there is an increase in the basal space between such layers (Fig. 4a) and the functional groups of the salt are electrostatically compatible to the starch structure (Coativy et al., 2015; Xie et al., 2013). In this sense, it is observed a greater tortuosity to the passage of the molecules of water vapor along the exfoliated bionanocomposite matrix, resulting in the low WVP of the biofilm A.

3.2.2. Fourier transform by infrared radiation - FTIR

The FTIR was used to identify the possible interactions established between cassava starch, glycerol and OBent-Ca. The spectra of biofilms A and B are shown in Fig. 5.

In Fig. 5, the wide absorption band, corresponding to the asymmetric stretching of O—H bonds between 3250 and 3455 cm^{-1}, is indicative of the presence of the intermolecular hydrogen bonds established in biofilms A and B (Liu et al., 2011; Romero-Bastida et al., 2016). According to Fig. 5, biofilm A presented such an elongated band when compared to biofilm B, proving that OBent-Ca is being used as a barrier to water vapor along the starch film by the occurrence of interaction with the biopolymeric matrix, thereby, minimizing the possibility of the starch to establish bonds with the environment, so that the WVP is reduced; In biofilm B, there is a greater vulnerability of the film in making connections with the environment, so that the highest WVP was observed. This fact can be explained by the use of OBent-Ca as a filling material which, through the surfactant tail, disperses throughout the cassava starch by establishing intermolecular bonds between the monomers of the starch granules, consequently a smaller amount of O—H in the formed bionanocomposite is observed. The biofilm B showed a lower elongation due to the higher concentration of free O—H groups, which may be due to the presence of glycerol in greater quantity and the absence of OBent-Ca (Chiu et al., 2014; Gao et al., 2014; Kotal & Bhowmick, 2015). Moreover, the transmittance bands observed around 2750 cm^{-1} correspond to the stretching of the hydrocarbon bonds (C—H) from the monomers that compose the extensive branched chain by hydroxyl groups formed between amylose and amylopectin (Matsuda et al., 2013).

3.2.3. Atomic force microscopy - AFM

The surface morphology of the cassava starch films was investigated using the AFM, as shown in Fig. 6, through a topographic study resulting from the atomic interaction between the constituents of biofilms A and B.

The AFM micrograph shows that the roughness height of the biofilm A (Fig. 6a), 284.28 nm, was lower when compared to the biofilm B roughness height (Fig. 6b), 322.57 nm. In this perspective, the lower

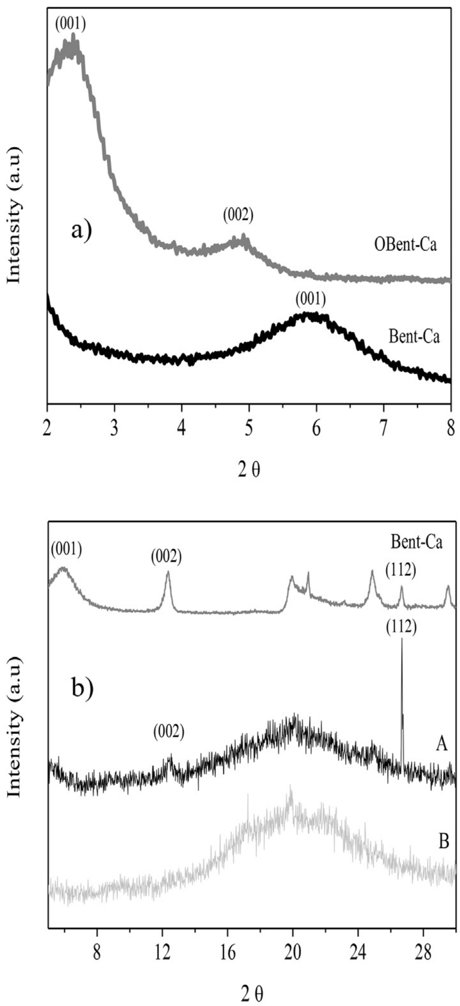

Fig. 4. Comparison of XRD patterns: (a) Bent-Ca and OBent-Ca (b) Biofilm of lower WVP (A), Biofilm of higher WVP (B) and Bent-Ca. Source: own authorship.

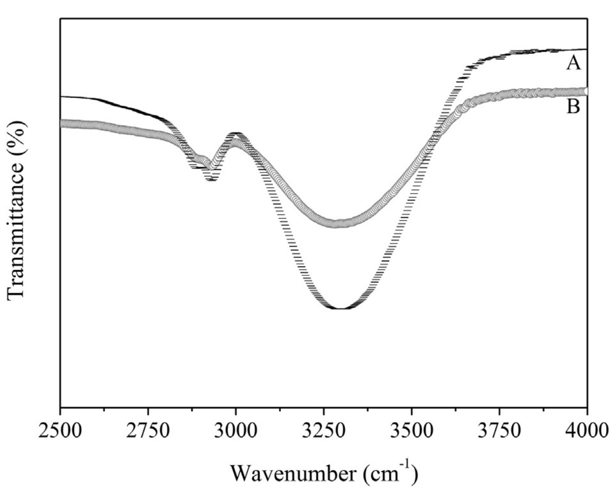

Fig. 5. Spectra of cassava starch films A and B.

roughness of the biofilm A may result from the formation of a bionanocomposite of starch and OBent-Ca, considering that in this condition the biopolymeric matrix presents a structure more ordered by establishing intermolecular bonds with the surfactant that modified the surface of the Bent-Ca, in this way the silicate layers that compose it are uniformly exfoliated at nano scale forming a cohesive biofilm and with

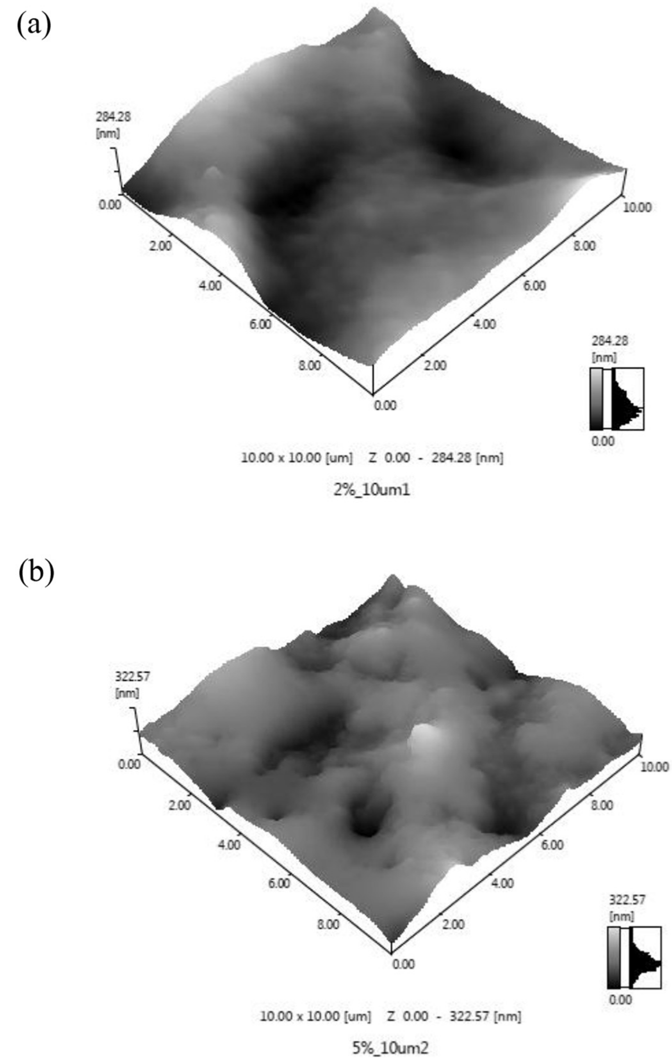

Fig. 6. AFM of cassava starch films: (a) Biofilm with lower WVP (A) and (b) Biofilm with higher WVP (B).

low WVP (Chivrac et al., 2010; Lavorgna et al., 2009). Such interaction is facilitated by the low glycerol concentration which according to (Muller et al., 2011) in this condition the plasticizer provides the necessary compatibility of the biopolymer with the filling material. Accordingly, the increased roughness of the biofilm B may be due to the high concentration of glycerol bound to the absence of the OBent-Ca resulting in a more disordered biopolymer structure and, therefore, more vulnerable to establishing hydrogen bonds with the water vapor molecules present in the environment, increasing the WVP (Casariego et al., 2009; Souza et al., 2012).

3.2.4. Scanning electron microscopy - SEM

SEM analyzes on cassava starch films (A and B) are shown in Fig. 7. Microscopy is used to visualize the homogeneity of the structural pattern of the biopolymeric matrix.

The images of SEM in biofilms A and B show that the presence of OBent-Ca as shown in Fig. 7a significantly influences the homogeneity of the starch film surface, making it more uniform without the presence of agglomerates along the biopolymeric matrix, as shown in Fig. 7b, which bring to the biofilm fragility fragments susceptible to water vapor permeability (Chiu et al., 2014; Kotal & Bhowmick, 2015).

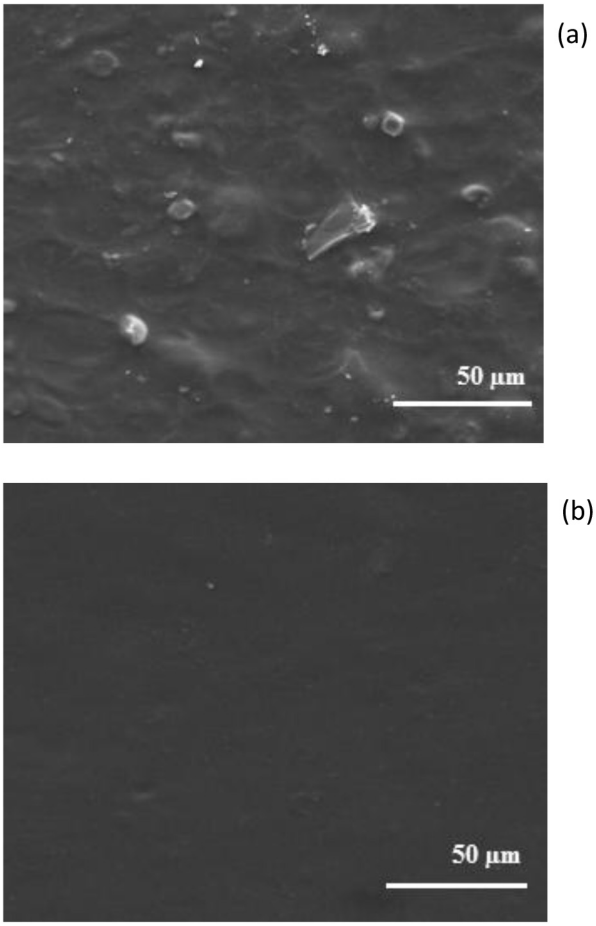

Fig. 7. SEM in cassava starch films with a magnitude of 1Kx: (a) Biofilm with lower WVP (A) and (b) Biofilm with higher WVP (B).

4. Conclusion

The modified clay was the factor of greater statistical significance on the WVP, being the factor that contributed to the improvement of the property of water vapor barrier. The factorial experiments showed that the interaction of the modified clay with both glycerol and cassava starch was significant for WVP reduction. The modified clay contributed to the reduction of the WVP, already the glycerol and the cassava starch for the increase. The possible interactions established between the constituents of the biofilms with both the lowest and the highest WVP were characterized by FTIR, AFM and SEM. The XRD confirmed the formation of a bionanocomposite exfoliated in the starch film with the lowest WVP, as well as the predominant presence of amylopectin in the composition of cassava starch, evidencing its semicrystalline structure and high hydrophilicity.

Acknowledgments

National Council for Scientific and Technological Development (CNPq); Post-graduate Program in Chemical Engineering (UFRN) and Post-Graduate Program in Materials Science and Engineering (UFERSA).

References

Abdel-Ghani, N. T., Hegazy, A. K., El-Chaghaby, G. A., & Lima, E. C. (2009). Factorial experimental design for biosorption of iron and zinc using *Typha domingensis* phytomass. *Desalination, 249*, 343–347.

Alboofetileh, M., Rezaei, M., Hosseini, H., & Abdollahi, M. (2013). Effect of montmorillonite clay and biopolymer concentration on the physical and mechanical properties of alginate nanocomposite films. *Journal of Food Engineering, 117*, 26–33.

ASTM E96/E96M-12 (1993). Standard test methods for water vapour transmission of materials. *Annual Book of Standards*.

Azarakhsha, N., Osmana, A., Ghazalia, H. M., Tanb, C. P., & Mohd Adzahanb, N. M. (2014). Lemongrass essential oil incorporated into alginate-based edible coating for shelf-life extension and quality retention of fresh-cut pineapple. *Postharvest Biology and Technology, 88*, 1–7.

Bingol, D., Tekin, N., & Alkan, M. (2010). Brilliant yellow dye adsorption onto sepiolite using a full factorial design. *Applied Clay Science, 50*, 315–321.

Casariego, A., Souza, B. W. S., Cerqueira, M. A., Teixeira, J. A., Cruz, L., Diaz, R., & Vicente, A. A. (2009). Chitosan/clay films' properties as affected by biopolymer and clay micro/nanoparticles' concentrations. *Food Hydrocolloids, 23*, 1895–1902.

Chiu, C. W., Huang, T. K., Wang, Y. C., Alamani, B. G., & Lin, J. J. (2014). Intercalation strategies in clay/polymer hybrids. *Progress in Polymer Science, 39*, 443–485.

Chivrac, F., Pollet, E., Dole, P., & Avérous, L. (2010). Starch-based nano-biocomposites: Plasticizer impact on the montmorillonite exfoliation process. *Carbohydrate Polymers, 79*, 941–947.

Coativy, G., Gautier, N., Pontoire, B., Buléon, A., Lourdin, D., & Leroy, E. (2015). Shape memory starch–clay bionanocomposites. *Carbohydrate Polymers, 116*, 307–313.

Cortez-Vega, W. R., Pizato, S., Souza, J. T. A., & Prentice, C. (2014). Using edible coatings from Whitemouth croaker (*Micropogonias furnieri*) protein isolate and organo-clay nanocomposite for improve the conservation properties of fresh-cut 'Formosa' papaya. Innov. *Food Science Emerging Technologies, 22*, 197–202.

Cyras, V. P., Manfredi, L. B., Minh-Tan, T. T., & Vazquez, A. (2008). Physical and mechanical properties of thermoplastic starch/montmorillonite nanocomposite films. *Carbohydrate Polymers, 73*, 55–63.

Gao, Y., Dai, Y., Zhang, H., Diao, E., Hou, H., & Dong, H. (2014). Effects of organic modification of montmorillonite on the performance of starch-based nanocomposite films. *Applied Clay Science, 99*, 201–206.

Hank, D., Azi, Z., Hocine, S. A., Chaalal, O., & Hellal, A. (2014). Optimization of phenol adsorption onto bentonite by factorial design methodology. *Journal of Industrial and Engineering Chemistry, 20*, 2256–2263.

Kotal, M., & Bhowmick, A. K. (2015). Polymer nanocomposites from modified clays: Recent advances and challenges. *Progress in Polymer Science, 51*, 127–187.

Lavorgna, M., Piscitelli, F., Mangiacapra, P., & Buonocore, G. G. (2009). Study of the combined effect of both clay and glycerol plasticizer on the properties of chitosan films. *Carbohydrate Polymers, 82*, 291–298.

Lee, S., Park, M., Kim, D., Kim, I. I., & Park, D. (2014). Catalytic performance of ion-exchanged montmorillonite with quaternary ammonium salts for the glycerolysis of urea. *Catalysis Today, 232*, 127–133.

Liu, H., Chaudhary, D., Yusa, S. I., & Tadé, M. O. (2011). Glycerol/starch/Na^+-montmorillonite nanocomposites: A XRD, FTIR, DSC and ^1H NMR study. *Carbohydrate Polymers, 83*, 1591–1597.

Matsuda, D. K. M., Verceheze, A. E. S., Carvalho, G. M., Yamashita, F., & Mali, S. (2013). Baked foams of cassava starch and organically modified nanoclays. *Industrial Crops and Products, 44*, 705–711.

Monteiro, M. K. S., Oliveira, V. R. L., Santos, F. K. G., Leite, R. H. L., Aroucha, E. M. M., Silva, R. R., & Silva, & K.N. de O. (2017). Analysis of water barrier, mechanical and thermal properties of nanocoposites based on cassava starch and natural clay or modified by anionic exchange. *Materials Research*.

Muller, C. M. O., Laurindo, J. B., & Yamashita, F. (2011). Effect of nanoclay incorporation method on mechanical and water vapor barrier properties of starch-based films. *Industrial Crops and Products, 33*, 605–610.

Palanikumara, K., & Davim, J. P. (2009). Assessment of some factors influencing tool wear on the machining of glass fibre-reinforced plastics by coated cemented carbide tools. *Journal of Materials Processing Technology, 209*, 511–519.

Pascall, M. A., & Lin, S. J. (2013). The application of edible polymeric films and coatings in the food industry. *Food Process Technology, 4*, 116.

Qi, G., Li, N., Sun, X. S., Shi, Y. C., & Wang, D. (2016). Effects of glycerol and nanoclay on physiochemical properties of camelina gum-based films. *Carbohydrate Polymers, 152*, 747–754.

Reddy, M. M., Vivekanandhan, S., Misra, M., Bhatia, S. K., & Mohanty, A. K. (2013). Biobased plastics and bionanocomposites: Current status and future opportunities. *Progress in Polymer Science, 38*, 1653–1689.

Restrepo-Flórez, J., Bassi, A., & Thompson, M. R. (2014). Microbial degradation and deterioration of polyethylene - A review. *International Biodeterioration & Biodegradation, 88*, 83–90.

Rhim, J. W., Park, H. M., & Hac, C. S. (2013). Bio-nanocomposites for food packaging applications. *Progress in Polymer Science, 38*, 1629–1652.

Romero-Bastida, C. A., Bello-Pérez, L. A., Velazquez, G., & Alvarez-Ramirez, J. (2015). Effect of the addition order and amylose content on mechanical, barrier and structural properties of films made with starch and montmorillonite. *Carbohydrate Polymers, 127*, 195–201.

Romero-Bastida, C. A., Tapia-Blácido, D. R., Méndez-Montealvo, G., Velázquez, G., & Ramirez, A. (2016). Effect of amylose content and nanoclay incorporation order in physicochemical properties of starch/montmorillonite composites. *Carbohydrate Polymers, 152*, 351–360.

Souza, A. C., Benze, R., Ferrão, E. S., Ditchfield, C., Coelho, A. C. V., & Tadini, C. C. (2012). Cassava starch biodegradable films: Influence of glycerol and clay nanoparticles content on tensile and barrier properties and glass transition temperature. *LWT - Food Science and Technology, 46*, 110–117.

Tan, B., & Thomas, N. L. (2016). A review of the water barrier properties of polymer/clay and polymer/grapheme nanocomposites. *Journal of Membrane Science, 514*, 595–612.

Velickova, E., Winkelhausen, E., Kuzmanova, S., Moldao-Martins, M., & Alves, V. D. (2013). Characterization of multilayered and composite edible films from chitosan and beeswax. *Food Science and Technology International, 21*(2), 83–93.

Wihodo, M., & Moraru, C. I. (2013). Physical and chemical methods used to enhance the structure and mechanical properties of protein films: A review. *Journal of Food Engineering, 114*, 292–302.

Xie, F., Pollet, E., Halley, P. J., & Avérous, L. (2013). Starch-based nano-biocomposites. *Progress in Polymer Science, 38*, 1590–1628.

Zhu, F. (2015). Composition, structure, physicochemical properties, and modifications of cassava starch. *Carbohydrate Polymers, 122*, 456–480.